Preferred citation: S. Heyden and P.J. Gustafsson. Stress-strain Performance of Paper and Fluff by Network Modelling. In **The science of papermaking**, *Trans. of the XIIth Fund. Res. Symp. Oxford, 2001*, (C.F. Baker, ed.), pp 1385–1401, FRC, Manchester, 2018. DOI: 10.15376/frc.2001.2.1385.

STRESS–STRAIN PERFORMANCE OF PAPER AND FLUFF BY NETWORK MODELLING

Susanne Heyden and Per Johan Gustafsson

Division of Structural Mechanics, Lund Institute of Technology
Lund University, Box 118, S-221 00 Lund, Sweden

ABSTRACT

The stress-strain performance of 2D and 3D cellulose fibre networks was simulated using a network model. A model network consists of bonded curled fibres placed at random in a cell. The bonds show a stick-slip fracture behaviour. Results concerning the influence of network density, fibre orientation and ductility of bonds on the stress–strain behaviour of a network are given, and an example of fracture localization is provided.

INTRODUCTION

Network models have been used for quite some time to yield the relations between micro- and macro-level properties of fibre networks. One reason for this is that knowledge about the connection between the micro-level properties and the corresponding global mechanical performance is crucial when it comes to understanding and also controlling the behaviour of fibre materials.

The earliest models used analytical methods and were thus confined to rather simple and uniform networks. Nevertheless they produced results of great interest and value. A landmark is the analytical fibre network model [1] presented by Cox in 1952. Cox assumed a perfectly homogeneous network of long straight thin fibres and derived the elastic constitutive parameters, for

2D and 3D networks. Other 2D models relying on the assumption of homogeneous strain that followed were [2–4]. However, more refined models are needed to provide realistic modelling of cellulose fibre networks. One approach that has been used [5,6] is to calculate the stress distribution in a single fibre as a function of orientation, length, degree of bonding etc, and integrate along a scan line over all possible values of the parameters. One problem is, though, that the integrals often become quite difficult to solve. In [6] this was overcome by generating random fibres crossing the scan-line and numerically evaluating the stresses.

As computer capacity has increased, network modelling has more and more become a matter of computer simulations, in which a random fibre network is generated and its properties analysed by means of the finite element method. This approach has primarily been used to model low-grammage paper [7–11]. There has also been development concerning what results come out of the simulations. The first few studies dealt with elastic stiffness only, Hamlen [8] studied the stress–strain relationship as a network breaks and Åström and Niskanen [9] extended the study of fracture of networks to include parameters as fracture behaviour and localization. Räisänen et al. [11] studied the behaviour of networks consisting of rigidly connected elastic-plastic fibres.

The previously mentioned computer simulation studies deal with planar networks, and close to planar 3D geometries have also been modelled [12]. In the present study [13], however, a network mechanics model is developed

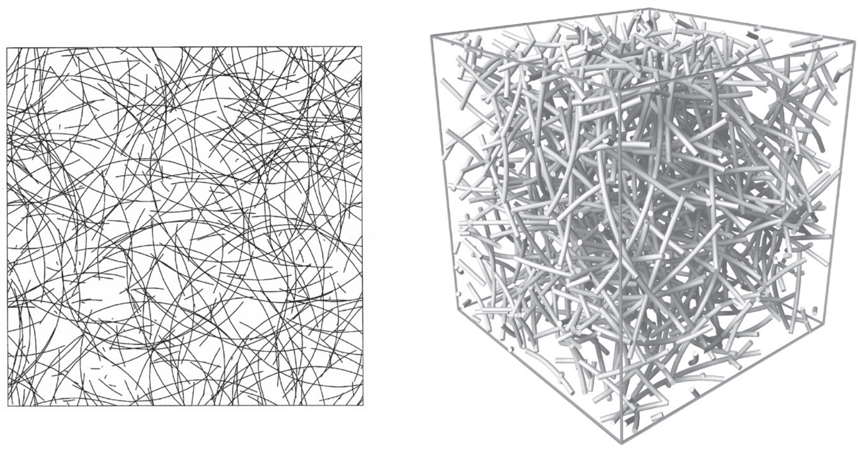

Figure 1 2D and 3D model networks.

which includes also a fully three-dimensional geometry. This means that both paper and fibre fluff, which is used in hygiene products, heat insulation and moulded products can be analysed.

The fibre networks were generated by placing fibres randomly in a cell. Figure 1 shows examples of 2D and 3D model networks. The networks were then analysed by means of the finite element method, and homogenized mechanical properties were obtained. The compliance and softening of the inter-fibre bonds are included in the model, a feature that is especially important when dry-shaped cellulose fibre fluff is considered. The simulated networks are of a periodic structure with cyclic boundary conditions along all boundaries, this is illustrated in Figure 4. This reflects the performance of a network of infinite size and enables a more consistent evaluation of the performance of the network. It is also possible to use a smaller network than would otherwise be the case. The output from the simulations includes elastic stiffness parameters and properties like strength, fracture energy and fracture softening that define the course of fracture.

MODEL

Figure 1 shows examples of 2D and 3D model networks. The model description will be focused on the 3D model as the 2D model is in most aspects a simpler variant of the 3D model. The bonds are, however, slightly different in 2D and 3D. A network consists of a cell of dimensions L_x, L_y, L_z, where fibres are placed at random, independently of each other. The network density, that is total fibre length per unit volume, is denoted ρ. The fibres are modelled as 3D linear elastic Bernoulli beams of constant curvature. They can be assigned arbitrary distributions in length (l_f), curl (c), cross sectional properties (area A_f, moments of inertia J_{zf}, J_{yf} and torsional rigidity, K_{vf}) and material stiffness (elastic modulus, E_f and shear modulus, G_f). The fibre orientation is governed by distribution functions N_α, N_β and N_γ, defining angle in the xy plane, out-of-plane angle and the angle of a curved fibre around its own axis.

Where the fibre centre lines are closer to each other than a distance e, there is a bond. A bond is modelled by an element consisting of two circular surfaces of area A_b connected by distributed normal and shear springs of stiffness k_n and k_t. The circular surfaces are at zero distance from each other and are rigidly connected to the fibre centre lines. The bonds show a stick-slip fracture behaviour with the slip criterion shown in Figure 2. The slip criterion is defined in the normal stress – shear stress ($\sigma_n - \tau$) plane for the bond, by the initial adhesion strength σ_{adh} and the initial shear strength factor, μ. The

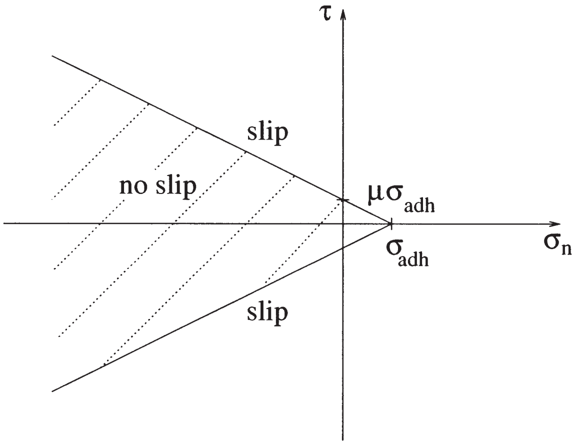

Figure 2 Slip criterion for 3D bond.

compressive normal stress part of the curve was experimentally verified by Andersson and Rasmuson [14]. A bond can slip at most n_s times and at each slip there is a degradation in stiffness and strength properties.

In a 2D network there is a bond wherever two fibres cross and a bond element consists of springs resisting translational relative movement between the fibres (k_x, k_y) and one spring resisting relative rotation (k_ϕ). The slip criterion for a 2D bond is

$$g(F, M) = \frac{|F|}{F_{ult}} + \frac{|M|}{M_{ult}} - 1 = 0, \tag{1}$$

where $|F|$ is the absolute value of the vector sum of the forces in the x and y springs, F_{ult} is the ultimate force of the bond, $|M|$ is the absolute value of the moment in the ϕ spring and M_{ult} is the ultimate moment of the bond. The degradation of a 2D bond element at a slip is illustrated in Figure 3. When a slip occurs, the stiffness is reduced by a factor λ_1 and the strength is reduced by a factor λ_2. This is repeated $n_s - 1$ times, and when $g(F, M) = 0$ the n_sth time the bond fails completely.

The studied network is a small part of the material, a representative cell. The global network geometry is assumed to be periodic, made up of many identical cells which are geometrically compatible, see Figure 4a. A set of

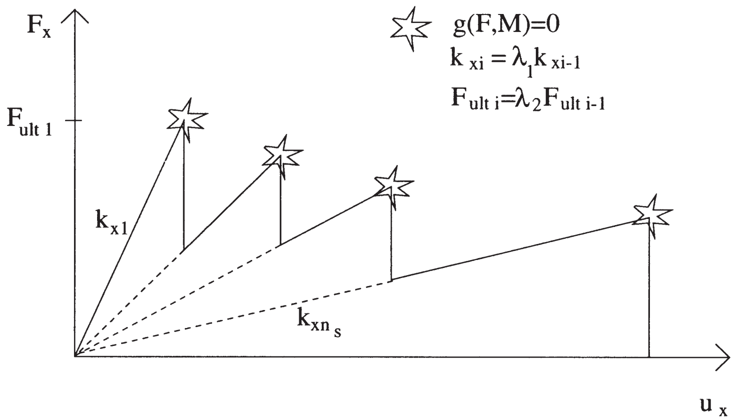

Figure 3 Stick-slip fracture performance of a 2D bond.

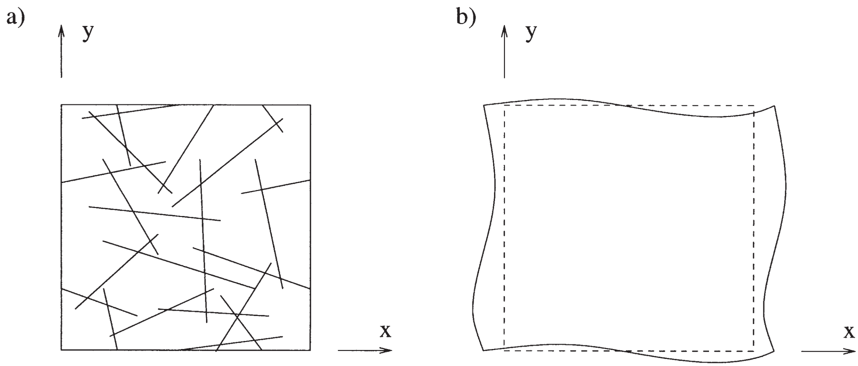

Figure 4 Example of a 2D periodic network geometry, where the opposite sides of the cell match. b) Network cell subjected to strain by means of periodic boundary conditions. Opposite sides match also after deformation even though the sides are not forced to remain straight.

periodic boundary and loading conditions is defined. These allow the boundaries of the cell to deform without affecting the compatibility of displacements. Figure 4b shows a symbolic example of a deformed 2D cell. An important effect of this approach is that local equilibrium is achieved for each point along the boundaries. The avoidance of constraints such as straight boundaries also facilitates obtaining relevant results even in the case of small network cells.

ANALYSIS

The mechanical behaviour of a network is analysed by the finite element method. The network cell is subjected to deformation and the corresponding forces on the boundaries are calculated. Due to non-linear properties and fracture of the bonds, the FE analysis is carried out as a series of linear steps. The primary result consists of corresponding load-deformation values through the loading history from zero load to complete fracture of the network. From the load-deformation values the stress–strain curves which are shown in the results section can easily be obtained by dividing with area and length of cell side respectively. The first point gives information about the elastic stiffness, and fracture-related parameters can be extracted from the complete curve. The obtained curves have a pronounced saw-tooth appearance. To facilitate interpretation of the figures the curves are replaced by hand-drawn approximate mean curves. Due to the random character of network structures, several nominally equal structures are in general simulated in order to get representative mean values and standard deviations.

If six different load-cases, corresponding to the six modes of unit strain (3D), are analysed, the homogenized isotropic, orthotropic or transversely isotropic elastic parameters can be obtained by a least square method, as is shown in [13].

Parameters such as strength and fracture energy are evaluated in a simple manner from the load-deformation curve. The results of the FE analysis also make it possible to study the general fracture mechanisms of the network, and in particular the development of a localized fracture process region.

STRESS–STRAIN PERFORMANCE RESULTS

Simulations were made to evaluate the influence of different micro-level parameters on the global mechanical performance. The influence of network density, in-plane and out-of-plane fibre orientation distribution and ductility of bonds will be shown in the following. An example of fracture localization will also be given. The set of input values in Table 1 was used in the simulations, where nothing else is said. The 3D network shown in Figure 1 was also generated using these input values.

The influence of network density on the fracture behaviour of 2D and 3D networks has been examined. The behaviour of a series of 2D networks of densities $\rho = 8.7$, 15 and 20 mm^{-1} and a series of 3D networks of densities $\rho = 75$, 87.5, 100, 112.5, 125 and 137.5 mm^{-2} was simulated. The networks were subjected to increasing strain in the x-direction and zero strain in the

Table 1 Input parameters which were used for the simulations where nothing else is stated.

Parameter	Value and unit-2D	Value and unit-3D
Fibre length l_f	1 mm	1 mm
Fibre curl c	1	0.91
Fibre cross section area A_f	$2.5 \cdot 10^{-10}$ m^2	$2.5 \cdot 10^{-10}$ m^2
In-plane moment of inertia J_{zf}	$2.0 \cdot 10^{-21}$ m^4	$2.0 \cdot 10^{-21}$ m^4
Out-of-plane moment of inertia J_{yf}	–	$2.0 \cdot 10^{-21}$ m^4
Fibre torsional rigidity K_{vf}	–	$3.5 \cdot 10^{-21}$ m^4
Fibre elastic modulus E_f	$35 \cdot 10^9$ Pa	$35 \cdot 10^9$ Pa
Fibre shear modulus G_f	–	$2.6 \cdot 10^9$ Pa
Bond area A_b	–	$3.1 \cdot 10^{-10}$ m^2
Bond normal stiffness k_n	–	$3.0 \cdot 10^{13}$ Pa/m
Bond shear stiffness k_t	–	$3.0 \cdot 10^{12}$ Pa/m
Initial adhesion strength σ_{adh}	–	$5 \cdot 10^5$ Pa
Initial shear strength factor μ	–	0.5
Bond transl. stiffness $k_{x1} = \mathrm{k}_{y1}$	8750 N/m	–
Bond rotational stiffness $k_{\phi 1}$	$2.8 \cdot 10^{-7}$ Nm/rad	–
Initial ultimate force F_{ult}	$3.5 \cdot 10^{-3}$N	–
Initial ultimate moment M_{ult}	$5.6 \cdot 10^{-9}$ Nm	–
Reduction of stiffness at slip λ_1	1	1
Reduction of strength at slip λ_2	1	1
Slips before complete failure n_s	1	1
Cell size L_x, L_y, L_z	1.2 mm	1.2 mm
Network density ρ	60 mm $^{-1}$	145 mm^{-2}
Distr. of in-plane fibre angle N_a	$\frac{1}{\pi}$, $0 < \alpha < \pi$	$\frac{1}{\pi}$, $0 < \alpha < \pi$
Distr. of out-of-plane fibre angle N_β	–	$\cos\beta$, $0 < \beta < \pi/2$
Distr. of angle around fibre axis N_γ	–	$\frac{1}{\pi}$, $0 < \gamma < \pi$
Largest distance for bond e	–	$20 \cdot 10^{-6}$ m

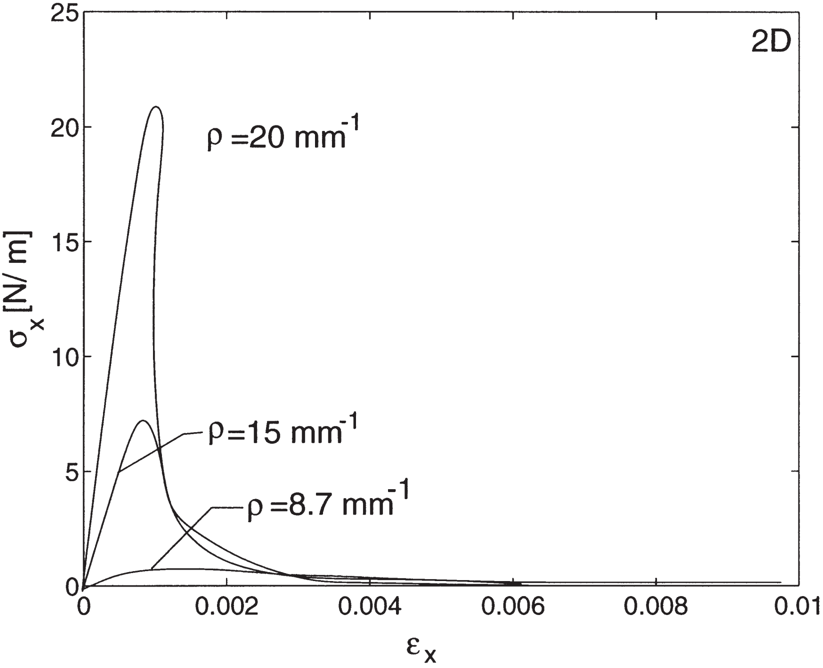

Figure 5 Stress-strain relationships for 2D networks of different densities.

y- (and z-) direction(s). Five simulations were performed for each value of network density and the averages of the stress-strain relationships for the different densities are given in Figures 5 and 6. As ρ increases, the 2D networks become considerably stronger, and also more brittle. Also for 3D, as ρ increases the networks become stronger, they reach maximum stress at a lower strain and the curves show a steeper descent after maximum load. 2D and 3D networks show in principle the same behaviour with respect to change in density. The simulated 2D networks are, however, more brittle despite the lower numerical values of the density since a certain total fibre length per square metre constitutes a much denser network, in terms of free fibre segment length, than the same total length of fibres distributed in a cubic meter.

The influence on the elastic stiffness of a non-uniform orientation distribution of the fibres was investigated. Two different kinds of non-uniform orientation distributions were studied; 2D networks where there is a preference for one fibre direction in the plane, and 3D networks where the fibres tend to lie

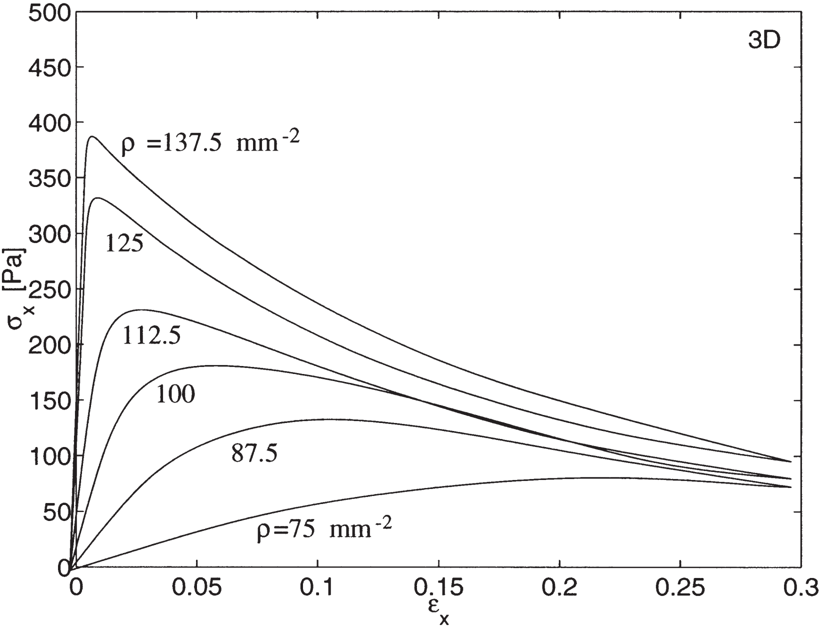

Figure 6 Stress-strain relationships for 3D networks of different densities.

in one plane. A non-uniform in-plane orientation distribution was defined as

$$N_a = \frac{1}{\pi} - a\cos 2\alpha, \tag{2}$$

where a is a constant representing the degree of anisotropy. 2D simulations were performed for the cases of $a = 0$, $1/(2\pi)$ and $1/\pi$. Figure 7 shows examples of network geometries for the three different values of a. For each value of a, 10 simulations were performed of nominally identical networks, and orthotropic material parameters were evaluated. Ideally, E_x and E_y should be identical for $a = 0$. That they are not is due to the limited number of networks analysed and the difference is not statistically significant. As a increases there is a stronger tendency for the fibres to be oriented vertically, as can be seen from Figure 7. This results in an increasing modulus E_y and decreasing E_x, as can be seen in Figure 8, where the mean values and standard

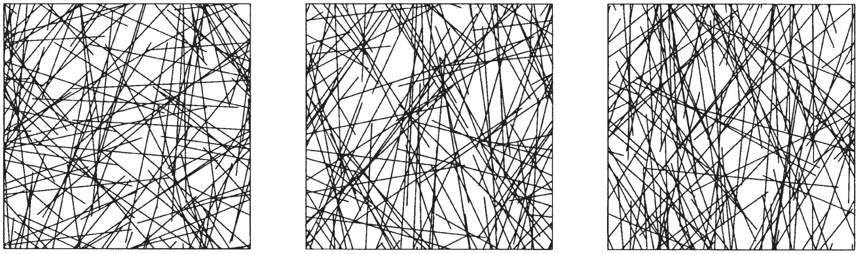

Figure 7 Examples of network geometries for the cases a = 0, a = 1/(2π) and a = 1/π.

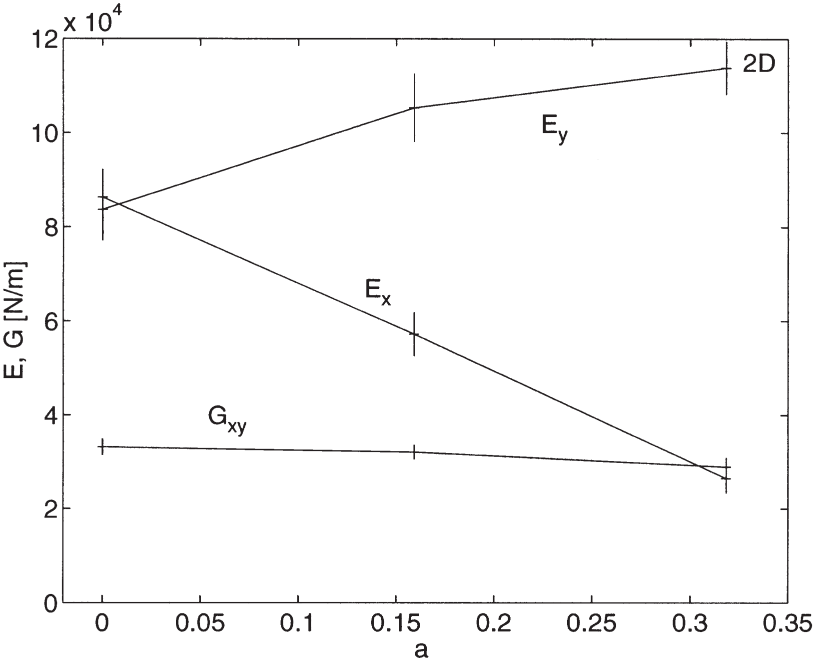

Figure 8 Elastic moduli plotted against orientation distribution parameter, a.

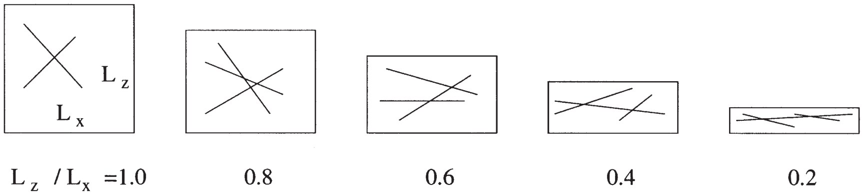

Figure 9 Investigated 3D cell shapes. $L_z = l_y$ for all cells.

deviation of E_x, E_y and G_{xy} are indicated. The shear modulus, G_{xy}, decreases only slightly as a increases.

Simulations were also performed on 3D networks with a non-uniform orientation distribution. A series of cells ranging from a cube, where $L_x = L_y = L_z$, to a cell that is compacted in the z-direction and thus approaching a 2D network was studied. The distribution of the out-of plane fibre angle β was set to:

$$N_\beta = \frac{L_x}{L_z}\cos\beta \quad 0 \le \beta \le \arcsin\frac{L_z}{L_x}. \tag{3}$$

Figure 9 shows symbolically the five types of network cells investigated. The number of fibres was 173 in all the cells. This corresponds to a network density of 100 mm^{-2} for the case of $L_z/L_x = 1.0$, and a density of 500 mm^{-2} when $L_z/L_x = 0.2$. The simulations can be viewed as an illustration of how the network properties change when a fixed number of fibres form a network which ranges from a full 3D network to close to a 2D network. The material properties were evaluated as for a transversely isotropic material. The parameters given in Figure 10 are in-plane and out-of-plane elastic modulus, showing the average of ten simulations. As the network is compacted the fibres become more oriented in the xy-plane giving an increased stiffness in this plane. The number of inter-fibre bonds also increases, making the fibre segments shorter and thus decreasing the influence of bending and torsion. These two effects result in an extremely high increase in in-plane stiffness. The out-of-plane stiffness also shows an increase as the ratio L_z/L_x decreases. This implies that the effect of shorter fibre segments is more important than that of fewer fibres being oriented in the z-direction. The ratio $E_{in\text{-}plane}$ to $E_{out\text{-}of\text{-}plane}$ is 0.8 at $L_z/L_x = 1.0$ and 44 at $L_z/L_x = 0.2$. At $L_z/L_x = 1.0$ the ratio should ideally be equal to 1.0; this was not so, due to the considerable spread in the results at this low density. The coefficients of variation from the simula-

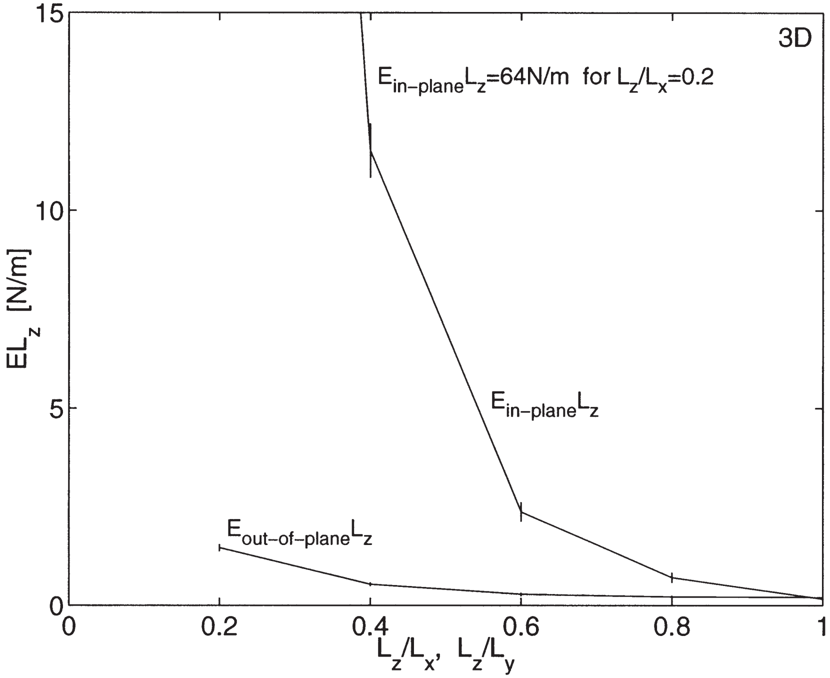

Figure 10 EL_z plotted against $L_z/L_x = L_z/L_y$.

tions range from approximately 0.35 for $L_z/L_x = 1.0$ down to 0.10 for $L_z/L_x = 0.2$.

For L_z/L_x ratios of 1.0 and 0.8 it was possible to follow the entire fracture process. Networks with smaller L_z/L_x ratios was not simulated since the number of degrees of freedom increases rapidly as the network is compressed. Five networks for each L_z/L_x ratio were simulated and were subjected to uniaxial tension in the *x*-, *y*- and *z*-directions, each simulation starting from an undamaged network.

The results are shown in Figure 11. Since the results for the three different loading directions are approximately equal for the $L_z/L_x = 1.0$ networks, the stress–strain curves representing uniaxial strain in the three different directions are plotted as one curve in Figure 11. For the networks where $L_z/L_x = 0.8$, the same applies to strain in the *x*- and *y*-directions, and these results are presented as one curve in Figure 11. Straining in the *z*-direction gives, however, different results and is represented by the middle curve in the figure.

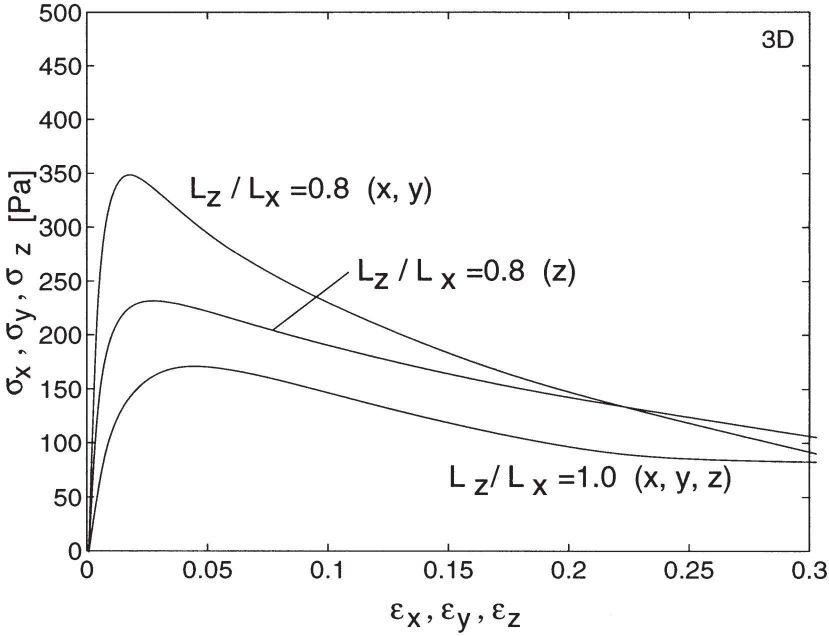

Figure 11 Stress–strain relationship for networks with different values of L_z/L_x and strain in different directions.

When the same number of fibres form a network in a cell of smaller height, and the fibres have a stronger tendency to be oriented in a plane, more bonds are formed and the free fibre segments become shorter. This gives an effect on the stress–strain curve similar to that of higher network density, where the maximum stress is higher and is reached at a lower level of strain. The $L_z/L_x = 0.8$ networks also become stronger for strain in the *z*-direction, indicating that the effect of shorter fibre segments is more important than the fact that fewer fibres are oriented in the *z*-direction, as was also the case for initial stiffness.

Simulations have also been made in order to investigate the influence of the ductility of bonds on the global fracture behaviour of a 2D network. The stick-slip behaviour of the bonds is defined in Figure 3. The parameters used were reduction in stiffness between two slips $\lambda_1 = 0.5$, and reduction in strength between two slips $\lambda_2 = 1.0$. The number of slips investigated before complete failure, n_s, were 1, 2 and 5, and the network density was 20 mm^{-1}. As

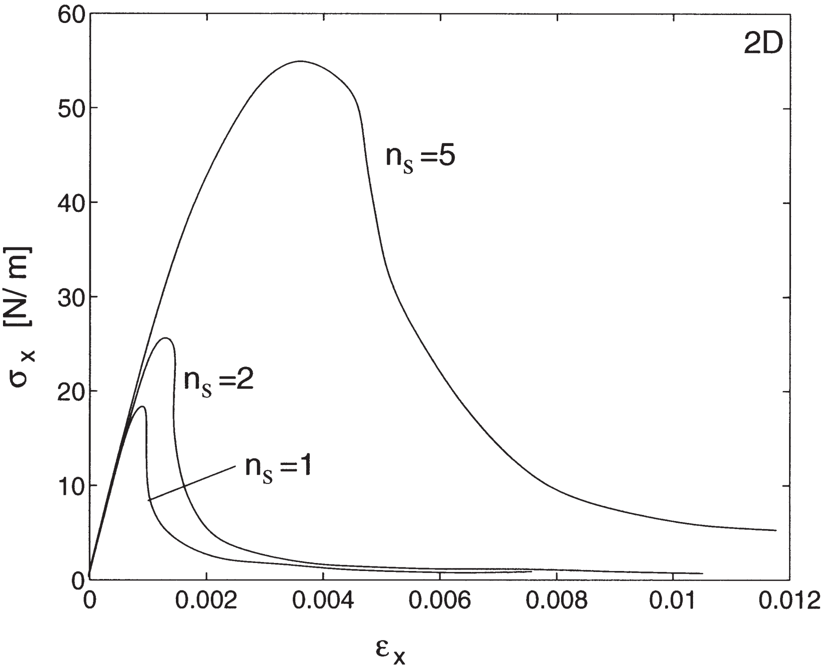

Figure 12 Stress–strain relationships for $n_s = 1$, 2 and 5.

many as five slips before final failure of a bond may seem a lot, but the relative displacement of two fibres in a bond here is still on the microscopic level. The effect of fibres slipping and forming new bonds in a new geometric configuration remains to be accounted for. Two simulations were made for each value of n_s.

The results of the simulations are shown in Figure 12. It is clear that an increase in bond ductility has a remarkable effect on the global strength and fracture energy. This is because the greater ductility allows the degree of utilisation to become more evenly distributed over the network. The stiffness of a bond that is severely stressed is reduced, allowing other less stressed bonds to take over part of the load. Ideally, one could imagine a situation where every bond in the network reaches final failure at the same time, although this would cause a very abrupt failure. This strong effect of bond ductility was not found in 3D networks, probably because the density is often so low in this kind of material that the potential for redistribution of load within the network is limited.

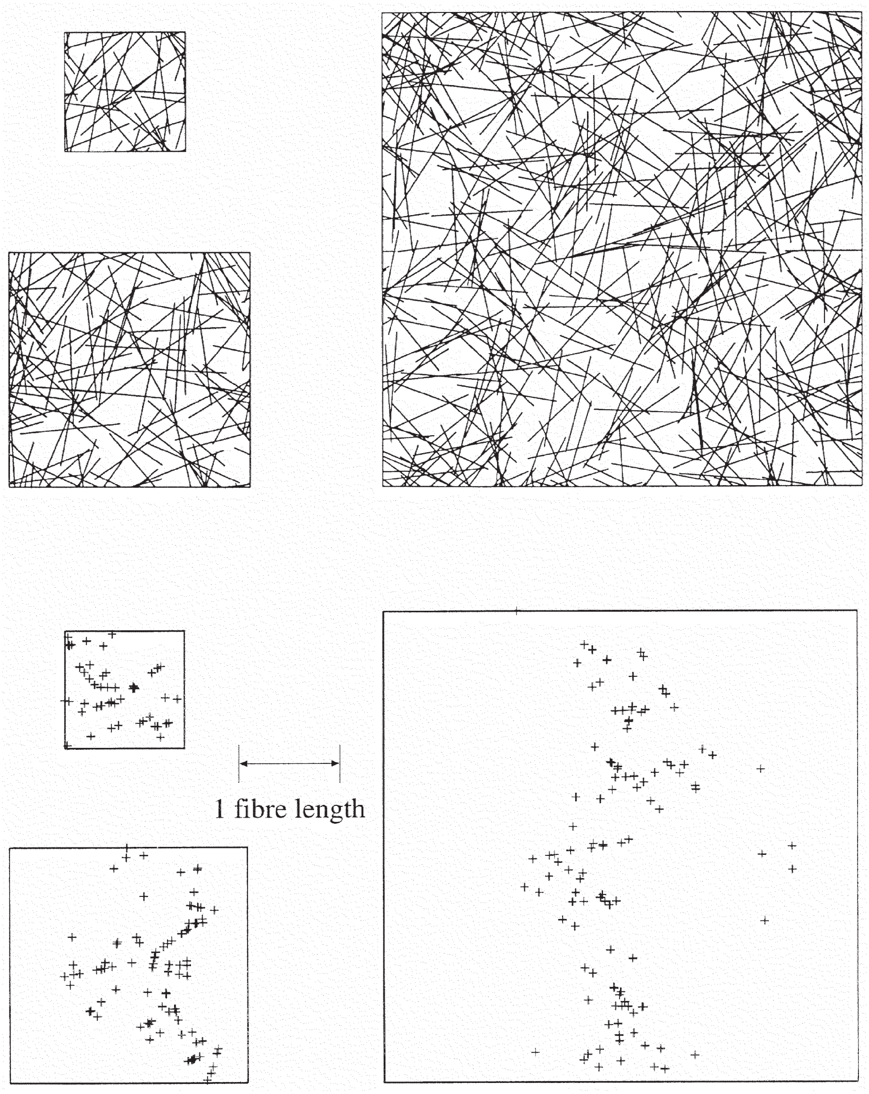

Figure 13 Networks and locations of fractured bonds.

When a network fails the local bond or fibre failures tend to be localized in a fracture zone which develops into a crack at complete failure. This localization phenomenon, which often is initiated at maximum load has been studied for 2D networks. Figure 13 shows examples of networks and locations of the fractured bonds for the three different sample sizes, $L/l_f = 1.2$, 2.4 and 4.8. It can be seen from the figure that the fracture process zone is of the same order of magnitude as the fibre length. Hence, in the smallest network in which $L/l_f = 1.2$, one cannot distinguish a localized fracture zone since the entire area under observation represents a fracture zone. If one wishes to study localization phenomena, the dimensions of the cell studied should therefore be well over one fibre length. The sample size also affects the shape of the stress–strain curve of a network. It is due to the small sample size that the descending part of the stress–strain curve can be studied, for larger cells as well as test specimens release of the elastic energy stored in the network will give a more brittle failure.

CONCLUSIONS

A 3D network model was proposed and implemented. This makes it possible to study the mechanical behaviour of low-density papers and dry-shaped cellulose fibre fluff by means of computer simulations. Parameter studies have been performed in order to reveal the influence of various micro-level parameters on the geometry structure, elastic stiffness and fracture behaviour on the global level. The results obtained contribute to the understanding of the prevailing mechanisms of a fibrous network, and the model also offers the possibility of further investigations concerning the influence of different micro-level variables.

ACKNOWLEDGEMENTS

Financial support from the Foundation for Strategic Research (Forest Products Industry Research College Programme) and Bo Rydin's foundation for scientific research is gratefully acknowledged.

REFERENCES

1. Cox, H.L., "The elasticity and strength of paper and other fibrous materials", *British Journal of Applied Physics*, **3**: 72–79 (1952).
2. Van den Akker, J.A., "Some theoretical considerations on the mechanical proper-

ties of fibrous structures", in: Trans. Brit. Paper and Board Makers' Assoc. Sympos. Consol. Paper Web, pp. 205–241, London (1962).
3. Perkins, R.W. and Mark, R.E., "On the structural theory of the elastic behavior of paper", *Tappi J.*, **59**(12): 118–120 (1976).
4. Page, D.H., Seth, R.S. and De Grace, J.H., "The elastic modulus of paper: Parts 1–3, *Tappi J.*, **62**(9): 99–102 (1979); **63**(6): 113–116 (1980); **63**(10) 99–102 (1980).
5. Kärenlampi, P., "Effect of Distributions of Fibre Properties on Tensile Strength of Paper, A Closed-Form Theory", *J. Pulp and Paper Sci.*, **21**(4): J138–J143 (1995).
6. Feldman, H., Jayaraman, K. and Kortschot, M.T., "A Monte Carlo Simulation of Paper Deformation and Failure", J. *Pulp and Paper Sci.*, **22**(10): J386–J392 (1996).
7. Rigdahl, M., Westerlind, B. and Hollmark, H., "Analysis of cellulose networks by the finite element method", *Journal of Materials Science*, **19**: 3945–3952 (1984).
8. Hamlen, R.C., "Paper structure, mechanics, and permeability: Computer–aided modeling", Ph.D. thesis, University of Minnesota, USA (1991).
9. Åström, J.A. and Niskanen, K.J., "Symmetry-Breaking Fracture in Random Fibre Networks", *Europhys. Lett.*, **21**(5): 557–562 (1993).
10. Jangmalm, A. and Östlund, S., "Modelling of curled fibres in two-dimensional networks", STFI, Stockholm, Sweden (1995).
11. Räisänen, V.I., Alava, M.J., Nieminen, R.M. and Niskanen, K.J., "Elastic-plastic behaviour in fibre networks", *Nordic Pulp and Paper Research Journal*, **4** (1996).
12. Stahl, D.C. and Cramer, S.M., "A Three-Dimensional Network Model for a Low Density Fibrous Composite", *J. Engineering Materials and Technology*, **120**: 126–130 (1998).
13. Heyden, S., "Network Modelling for the Evaluation of Mechanical Properties of Cellulose Fibre Fluff", Report TVSM-1011, Doctoral Thesis, Lund University, Division of Structural Mechanics, Lund, Sweden (2000).
14. Andersson, S.R. and Rasmuson, A., "Dry and Wet Friction of Single Pulp and Synthetic Fibres", *Journal of Pulp and Paper Science*, **23**(1): J5–J11 (1997).

Transcription of Discussion

STRESS–STRAIN PERFORMANCE OF PAPER AND FLUFF BY NETWORK MODELLING

Susanne Heyden and Per Johan Gustafsson

Division of Structural Mechanics, Lund Institute of Technology

Al Button Buttonwood Consulting

I really like your model, a nice combination of (a) you can manipulate the element and (b) you can put it all together. Here are my thoughts about your description of the bonds and how they behave. You describe them a circular and I assume that you make an assumption about the change in the area of the bonds as you go through the various steps of slip. Since you are assuming linear elastic fracture mechanics behaviour, unless you get a change in the width of the bond, you were not likely to see a change in the actually strength of the bond. I have done work on the fibre-to-fibre bonds. They will crack, the cracks will progress, and you will get a reduced modulus.

Susanne Heyden

No, I don't assume that the bond area decreases but the stiffness and strength of the bond changes during loading.

Al Button

Unless you get an actual reduction in the width of bond in the primary direction of loading, you are not likely to see a change in actual strength. You will see a change in modulus, but until that width gets reduced in someway it will probably have the same strength. You have go to a critical level of stress before you get failure, so as long as you have that crack front width and intensification and enough area to carry that intensification, the bond will keep the same strength.

Discussion

Jean-Claude Roux EFPG

I would like you to comment on the fact that you used simulation strain of about 20–30% at the right part of your Figure 6. What about the use of the logarithmic compressive strain, you don't use it in your simulations, can you comment on this?

Susanne Heyden

I didn't study compression at all. If you want to study compressive straining of a material it is more complicated in many ways you have instabilities like buckling and new bonds will probably be formed I only simulate tension, but still the large strains are a problem and at the right end the curves are not entirely clear.

Derek Page Institute of Paper Science & Technology

You put in a bond shear modulus or some property of the bonding shear – but a bond has no thickness how can any deformation come from a contact area which has no thickness.

Susanne Heyden

It is a fictitious bond model. The idea has been to have a model that takes into count several effects, but there is not a direct physical resemblance to what is really happening.